

Discontinuous Weighted Least-Squares Approximation on Irregular Grids

N.B.Petrovskaya¹

Abstract: Discontinuous weighted least-squares (DWLS) approximation is a modification of a standard weighted least-squares approach that nowadays is intensively exploited in computational aerodynamics. A DWLS method is often employed to approximate a solution function over an unstructured computational grid that results in an irregular local support for the approximation. While the properties of a weighted least-squares reconstruction are well known for regular geometries, the approximation over a non-uniform grid is not a well researched area so far. In our paper we demonstrate the difficulties related to the performance of a DWLS method on distorted grids and outline a new approach based on a revised definition of distant points on distorted grids. Our discussion is illustrated by examples of DWLS approximation taken from computational aerodynamics problems.

Keyword: discontinuous weighted least-squares approximation, stretched mesh, outliers

1 Introduction

A least-squares (LS) method is one of the most well known approaches in solving a problem of finding the best polynomial approximation to the input samples. Originally developed for statistical regression, a general concept of LS approximation nowadays is widely used for various applications beyond statistics.

While the LS approximation is a powerful tool for various process modeling, its accuracy is based on the assumption that all data points provide equally precise information. However, in many cases data point used for the LS method are of varying quality in terms of the uncertainty of the measurement.

Thus a widespread approach to improve the accuracy of a LS approximation is to use weights in the LS procedure [Björck (1996); Neter, Wasserman, Kutner (1985)]. The idea of a weighted LS approximation is to allocate weight coefficients to least-squares data in order to suppress data points where the observation error can be large. In many applications the uncertainty of the measurement is associated with geometrically distant points in the data set, so that the weight of each observation is often chosen to be a function of the inverse distance between two given points (e.g., see [Alexa, Behr, Cohen-Or, Fleishman, Levin and T. Silva (2003); Atluri, Kim, and Cho (1999); Bates, Watts (1988); Mavriplis (2003); Wendland (1995)]).

A discontinuous weighted least-squares (DWLS) approximation is a modification of a weighted LS method that has recently received a lot of attention in computational aerodynamics [Anderson, Bonhaus (1994); Barth (1991); Haselbacher (2006); Mavriplis (2007); Ollivier-Gooch, Van Altena (2002); Petrovskaya (2007)]. A DWLS method is a local weighted LS approximation that is computed separately at each point that belongs to a set of points selected over a computational grid. While this approach is loosely referred to as a 'weighed least-squares reconstruction' or just 'least-squares reconstruction' in computational aerodynamics [Anderson (1994); Barth (1991); Ollivier-Gooch, Nejat, Michalak (2007)], we use the name 'DWLS' in our paper in order to emphasize the local nature of the method. An accurate and computationally efficient local reconstruction of a given function at chosen grid points is an essential part of numerical solution to many computational aerodynamics problems. One basic application of the DWLS method is to reconstruct a solution gradient in projection-evolution discretization schemes that are heavily exploited

¹ School of Mathematics, University of Birmingham, Edgbaston, Birmingham, B15 2TT, The United Kingdom

in industrial aerodynamic codes. A second order accurate discretization requires the solution gradient reconstruction to maintain the accuracy of the scheme [Anderson, Bonhaus (1994); Barth, Jespersen (1989); Mavriplis (2007)]. The solution gradients should be reconstructed based upon a solution field at grid nodes, and the DWLS method is an attractive approach for this task, as it only requires local support to compute the gradient at a given grid point [Barth (1991); Haselbacher, Vasilyev (2003)].

A DWLS reconstruction is very similar to a moving least-squares (MLS) method [Lancaster, Salkauskas (1981)], where the coefficients of a LS approximation depend on the location of a point where the reconstruction is made. The MLS approximation is a well-known approach that has been successfully adapted in meshless methods such as a diffuse approximate method (DAM, [Nayroles, Touzot, Villon (1992)]) as an alternative to finite element methods in solution of various heat transfer and fluid flow problems [Prax, Sadat, Dabboura (2007); Sadat, Prax (1996); Šarler, Vertnik, Perko (2005)]. However, the difference between a DWLS and MLS procedure is that in the latter case a local support for the approximation is prescribed by the definition of a weight function in the problem [Levin (1998)], while for a DWLS approximation a local support (also called a reconstruction stencil) is entirely determined by the edge data structure of a computational grid. The weight function in a DWLS method is only used to improve the accuracy of the approximation on a given stencil by reducing the uncertainty of the measurement, as it has been mentioned above. Thus the formal definition of the DWLS method may involve a weight function given by the identity matrix ('unweighted reconstruction'), while the method will still benefit from a compact support at each computational point.

One basic feature of a DWLS reconstruction that stems from the nature of computational problems where the method is exploited is that a reconstruction stencil may present a highly irregular geometry because of generation of a non-uniform grid in the problem. For instance, the need for stretched

meshes may be dictated by a requirement of adequate resolution of the solution gradient in computational sub-domains around an airfoil. In particular, grid cells with very high cell aspect ratio inevitably appear as a result of grid generation in boundary layer regions. While the accuracy tests for a DWLS approximation on uniform and quasi-uniform meshes demonstrate very good results [Ollivier-Gooch, Van Altena (2002); Ollivier-Gooch, Nejat, Michalak (2007)], a reconstruction on irregular meshes presents a challenging and difficult problem as the method can lose accuracy to unacceptable limit [Mavriplis (2003); Petrovskaya (2007); Smith, Barone, Bond, Lorber, and Baur (2007)]. Let us notice here that a DWLS reconstruction task is an important part of a nonlinear solver used in a computational aerodynamics problem. Once the approximate solution has been reconstructed over the grid, the 'expanded' solution should be further used for the next nonlinear iteration that generally involves a discretization of governing equations as well as numerical solution of a resulting system of nonlinear algebraic equations. The poor accuracy of a DWLS reconstruction affects the convergence of the approximate solution by generating large discretization errors and ill-conditioned matrices. It has been demonstrated in [Mavriplis (2003); Smith, Barone, Bond, Lorber, and Baur (2007)] that the poor accuracy of the DWLS approximation may result in an oscillating inaccurate solution or even in a divergent solution.

A general problem of a weighted LS approximation on irregular meshes has received little attention in the literature so far (cf. the discussion in [Breitkopf, Naceur, Rassineux, and Villon (2005); Perko, Šarler (2007)]). A research effort in meshless methods that use the MLS approximation was mainly focused on the shape of weight functions to mitigate the impact of an irregular node distribution in the problem [Most, Bucher (2008)], where earlier results mainly dealt with heuristic determination of the geometric scaling of a weight function [Prax, Salagnac, Sadat (1998)]. Recently the optimization of a scaling parameter in a Gaussian weight function for the MLS based diffuse approximate method

was implemented in [Perko, Šarler (2007)] to allow the authors to solve a transient Burgers equation over a random node distribution. The problem of finding the optimal radius of the support for a spline weight function has been investigated in [Nie, Atluri, Zou (2006)].

Meanwhile, the optimal radius of the support cannot be implemented in a DWLS problem as the size of a reconstruction stencil is prescribed by a geometry of a computational mesh and distant points are unavoidable in a stencil on grids with high cell aspect ratios. Earlier insight into the problem attributed poor accuracy of the method on stretched meshes to the impact of remote points on the results of a DWLS reconstruction, so that inverse distance weighting has been recommended by many authors (*e.g.*, see [Anderson, Bonhaus (1994); Barth (1991); Haselbacher (2006); Ollivier-Gooch, Nejat, Michalak (2007)]). However, it recently turned out that weighting of stencil points is not efficient on anisotropic meshes used in practical computations. It has been discussed in [Petrovskaya (2007); Smith, Barone, Bond, Lorber, and Baur (2007)] that the results of a weighted LS reconstruction can be worse than those for an unweighted one. Hence the problem of a DWLS reconstruction on irregular meshes appeals for a more detailed discussion, and in our paper an attempt has been made to sort out basic issues related to the problem. In particular, it will be demonstrated in the paper that the use of a weight function in a DWLS approximation requires a thorough definition of distant points in the problem. Furthermore, the recognition of the distant points in a reconstruction stencil should not rely upon geometric shape of the stencil only, as their definition is based on the data used for the approximation. This statement will be discussed in the paper where we introduce a novel concept of numerically distant points in a DWLS reconstruction. We demonstrate a difference between geometrically distant points (r -outliers) and numerically distant points (U -outliers) and conclude that poor accuracy of a DWLS approximation is mainly due to the presence of U -outliers in a reconstruction stencil. Our approach is illustrated

by numerical examples.

2 The local least-squares solution reconstruction

Discontinuous weighted least-squares approximation can be considered as a modification of a weighted LS approximation that does not require continuity of fit functions. Thus for a discussion of a DWLS approximation we need to outline a weighted LS method first. Below we briefly recall the basic concepts related to the least-squares approximation.

2.1 The weighted least-squares approximation

Consider a two-dimensional domain Ω and a set of points $P_i = (x_i, y_i) \in \Omega, i = 1, \dots, N$. A least-squares approximation deals with data \mathbf{U} at points P_i , where $U_i = U(P_i)$ can be considered as a value of a continuous function $U(x, y)$ at a given point P_i . The data \mathbf{U} should be fitted to the function

$$u_{LS}(x, y) = \sum_{k=0}^M u_k \phi_k(x, y), \quad M < N, \quad (1)$$

where $\mathbf{u} = (u_0, u_1, u_2, \dots, u_M)$ are fitting parameters, and $\phi_k(x, y), k = 0, \dots, M$, are polynomial basis functions. The unknown parameters $\{u_k\}$ are determined in the LS method by seeking the minimum of the following merit function (*e.g.*, see [Neter, Wasserman, Kutner (1985); Press, Flannery, Teukolsky, and Vetterling (1996)]),

$$F^2 = \sum_{i=1}^N \left[U_i - \sum_{k=0}^M u_k \phi_k(P_i) \right]^2, \quad (2)$$

Taking partial derivatives with respect to the fitting parameters u_k to find out $\min_{\mathbf{u}} F^2$, we obtain $M + 1$ normal equations of the LS problem

$$\frac{\partial F^2}{\partial u_k} = 0, \quad k = 0, \dots, M.$$

The normal equations can be written in the matrix form as

$$\mathbf{A}^T \mathbf{A} \mathbf{u} = \mathbf{A}^T \mathbf{U}, \quad (3)$$

where the design matrix \mathbf{A} is as follows

$$A_{ij} = \phi_j(P_i), \quad i = 1, \dots, N, \quad j = 0, \dots, M.$$

Once a function $u_{LS}(x, y)$ has been reconstructed, we can define its value everywhere in the domain Ω by computing $u(P)$ for arbitrary point $P = (x, y) \in \Omega$.

Similarly, weighted LS approximation minimizes the following functional

$$F_w^2 = \sum_{i=1}^N w(\bar{P}, P_i) [U(P_i) - u(P_i)]^2,$$

where the weight function $w(\bar{P}, P)$ is defined for a fixed point $\bar{P} \in \Omega$. The normal equations now are as follows

$$\sum_{i=1}^N w(\bar{P}, P_i) \left[U_i - \sum_{j=0}^M u_j \phi_j(P_i) \right] \phi_k(P_i) = 0, \\ k = 0, \dots, M,$$

and the solution is

$$\mathbf{u} = \mathbf{A}_{wls}^{-1} \mathbf{b}_{wls},$$

where $\mathbf{A}_{wls} = \mathbf{A}^T \mathbf{W} \mathbf{A}$, $\mathbf{b}_{wls} = \mathbf{A}^T \mathbf{W} \mathbf{U}$, and a diagonal weight matrix \mathbf{W} is defined as

$$W_{ij} = \begin{cases} w(\bar{P}, P_i), & i = j, \quad i, j = 1, 2, \dots, N, \\ 0, & \text{otherwise.} \end{cases}$$

The choice of the weight function $w(\bar{P}, P_i)$ depends on a given problem under consideration. In surface approximation problems the weight function $w(\bar{P}, P)$ is often defined to mitigate the impact of distant points on the accuracy of the approximation. For this purpose the weight function is chosen as a function of Euclidian distance $r = \|\bar{P} - P\|$ between point \bar{P} and a given point P . In MLS problems, where a weight function is required to provide a compact support for the least-squares approximation, the Gaussian or the spline weight function is the most popular choice [Most, Bucher (2008); Nie, Atluri, Zou (2006); Perko, Šarler (2007)], but other weight functions can also be found in the literature [Alexa, Behr, Cohen-Or, Fleishman, Levin and T. Silva (2003); Wendland (1995)].

An important feature of the weighted LS approximation is that the solution \mathbf{u} becomes a function of \bar{P} , and the fitting parameters have to be recomputed for any new \bar{P} . The global approximation in

this case can be achieved by imposing additional conditions on the approximation, such as the requirement that the supports of the weight functions entirely cover the domain Ω .

On the contrary, a discontinuous weighted least-squares approximation remains a local approximation, and no additional conditions are required to reconstruct function $u(x, y)$ in the domain of interest. The method formulation is discussed below.

2.2 The discontinuous weighted least-squares approximation

Let a computational grid G be generated in the domain Ω . For the sake of our further discussion we consider grid G as a set of points $P_i = (x_i, y_i)$, $i = 1, 2, \dots, N_G$, supported with a certain data structure (i.e., grid edges, grid cells, etc.). An example of a non-uniform computational grid generated around an airfoil is shown in Fig. 1.

Let us assume that the global data vector $\mathbf{U}_G = (U_1, U_2, \dots, U_{N_G})$ is defined in G . We then define a discrete set of points \bar{P}_l , $l = 1, \dots, L$, over the grid G , where the data \mathbf{U}_G will be approximated at each \bar{P}_l . The definition of the set $\{\bar{P}_l\}$ is based on a given computational problem under consideration. For instance, the set $\{\bar{P}_l\}$ may coincide with a set of all interior nodes in grid G , while the vector \mathbf{U}_G is defined at cell centroid points (a cell-centered discretization scheme). Below we consider a case when \mathbf{U}_G is defined at nodes of grid G , and the set $\{\bar{P}_l\}$ is a set of all edge midpoints taken on G (a node-centered discretization scheme).

We now allocate a local support S_l for each point \bar{P}_l , where the definition of S_l depends on the set $\{\bar{P}_l\}$. In case that a point \bar{P}_l is the edge midpoint for a grid edge e_l , the support S_l is allocated as follows. The two nodes n_1 and n_2 that comprise the edge e_l are identified, and S_l consists of all nodes that belong to edges incident to the node n_1 or n_2 . Thus the support S_l appears as a subset of N grid nodes, $S_l \subset G$, chosen by a known rule for local LS approximation at point \bar{P}_l . An example of the local support for the edge midpoint \bar{P}_l is shown as set I in Fig. 2.

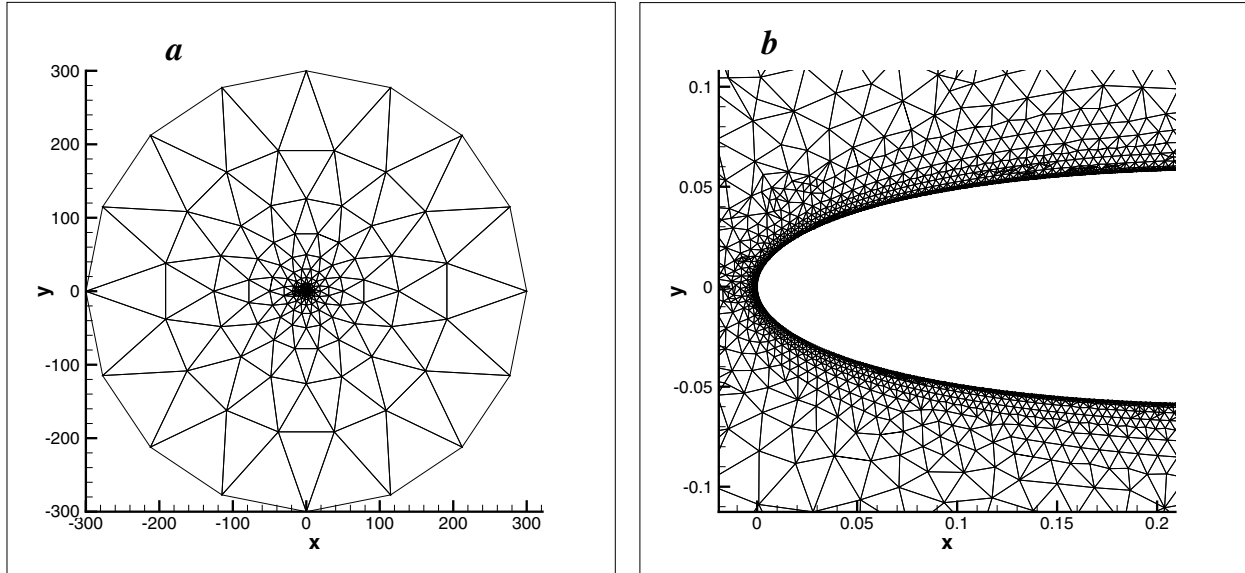


Figure 1: An unstructured computational grid around an airfoil. (a) A coarse quasi-uniform grid is generated in a far field. (b) A grid with high cell aspect ratios is required to resolve a solution near the wall.

Once the support S_l has been allocated, local numbering is used in the approximation problem. Namely, the point \bar{P}_l is now denoted as P_0 , and the support points are numbered as $P_i, i = 1, \dots, N$ (see Fig. 2), where the number N of support points can be different for two different points \bar{P}_{l_1} and \bar{P}_{l_2} , as it depends on the geometry of a computational grid. A widespread terminology is to use the name *reconstruction stencil* for the set S_l and to think of the LS approximation at point P_0 as of a *solution reconstruction* problem. The point P_0 is then called a central reconstruction node. This terminology comes from the fact that the data vector \mathbf{U}_G usually appears as an approximate solution computed at grid nodes and the solution \mathbf{U}_G should further be locally approximated (reconstructed) at some grid points.

Our next step is to allocate a local data vector $\mathbf{U} = (U_1, U_2, \dots, U_N)$ by taking the entries of \mathbf{U}_G at stencil points. We then implement a weighted LS approximation to reconstruct the solution at point P_0 . In our work we use the following weight function

$$w(P_0, P_i) \equiv w(r_{0i}) = r_{0i}^{-p}, p = 0, 1, 2, \dots, \quad (4)$$

where r_{0i} is the Euclidian distance between P_0 and $P_i, i = 1, 2, \dots, N$, and p is an integer polynomial

degree. The simple weight function (4) is a popular choice in computational aerodynamics problems [Barth (1991); Mavriplis (2003); Ollivier-Gooch, Van Altena (2002); Ollivier-Gooch, Nejat, Michalak (2007); Petrovskaya (2007)]. The unweighted reconstruction corresponds to $p = 0$, while $p > 0$ provides inverse distance weighting used to mitigate the impact of remote stencil points on the results of LS approximation.

A DWLS approximation does not require a user to assemble a global approximation over the domain Ω . Instead, we compute the approximation at each point P_l separately, and fit functions (1) remain discontinuous in Ω . Once the solution has been reconstructed at a given point \bar{P}_l , the next point \bar{P}_{l+1} is taken and the reconstruction procedure is repeated. At first glance, the entire algorithm can be considered as solving a number of weighted LS problems in domain Ω , where the results of each approximation can be considered independently. However, the nature of computational problems where a DWLS reconstruction is usually implemented dictates that the approximation at each point \bar{P}_l should be considered on a given computational grid G . That means the DWLS reconstruction has to deal with a pre-

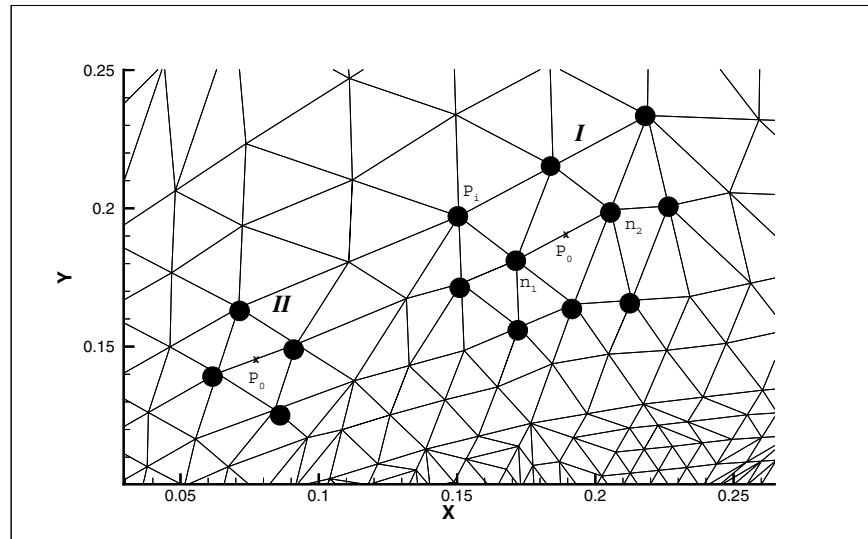


Figure 2: Examples of a reconstruction stencil for a DWLS approximation at point P_0 . Stencil members are shown as black circles. A stencil (I) consists of all grid nodes P_i ($i=1, \dots, 10$) that belong to edges incident to the node n_1 or n_2 . A compact stencil (II) consists of four grid nodes belonging to the adjacent cells that share a given edge.

scribed geometry of the support S_l that cannot be chosen from *a priori* considerations. The reconstruction stencil S_l is, in turn, entirely defined by the geometry of grid G . Thus the quality of the grid determines the accuracy of the DWLS approximation, as it will be discussed below.

2.3 The accuracy of the DWLS approximation on irregular meshes

A basic feature of a DWLS reconstruction is that the support S_l may present a highly irregular geometry. While for a standard weighted LS approximation the accuracy of the method can be assessed in many cases via smoothness of a reconstructed surface, with a DWLS approximation a user is concerned about the approximation error over a given set of points, no matter how many kinks and overlaps a resulting ‘surface’ may exhibit on the domain Ω . However, the accuracy of the DWLS approximation should be often achieved by using a distorted reconstruction stencil at each point \bar{P}_l . Most of the problems where a standard weighted LS approximation is employed allow a user to generate a regular grid to define the data set. Meanwhile, it is very of-

ten that highly irregular grids should be generated in computational problems where a DWLS reconstruction is used. For instance, grids with very high cell aspect ratios inevitably appear as a result of grid generation in boundary layer regions where the solution gradient should be adequately resolved. Below we discuss a typical example that well illustrates a DWLS reconstruction in computational aerodynamics problems.

Consider laminar flow around a Zhukovsky airfoil obtained as a result of numerical solution of the Navier-Stokes equations on a non-uniform unstructured grid [Johnson (2007)]. Let G_1 be a grid of $N_{G_1} = 12351$ nodes generated to resolve the solution in a boundary layer, so that the grid is quasi-uniform in a far field (see Fig. 1a) and has cells with big cell aspect ratios near the wall (Fig. 1b). A solution to the system of governing equations is computed by a numerical method (streamline upwind Petrov-Galerkin (SUPG), see [Hughes, Brooks (1979)]) that employs higher order polynomial functions to discretize the equations and results in an accurate solution on grid G_1 . In the discussed test case a solution has been obtained for a Mach number of 0.5, a Reynolds

number of 5000 and an angle of attack $\alpha = 0.0$. Characteristic boundary conditions have been implemented in a far field, and an isothermal solid wall boundary condition has been considered in a near field. The details of the numerical solution procedure can be found in [Venkatakrishnan, Allmaras, Johnson, and Kamenetskii (2003)].

In our study the first component of the velocity vector in the Navier-Stokes equations has been chosen as a scalar solution field $U(x, y)$ to discuss the DWLS reconstruction on grid G_1 . The solution obtained at grid nodes is used as a global data vector \mathbf{U}_G for a DWLS reconstruction of the solution at the edge midpoints on grid G_1 . The solution is reconstructed by a linear polynomial,

$$u_{DWLS}(x, y) = u_0 + u_1(x - x_0) + u_2(y - y_0), \quad (5)$$

and the weight function (4) with polynomial degree $p = 2$ is used for the reconstruction.

The grid G_1 , where the reconstruction has been made, is then uniformly refined, so that the edge midpoints on the original grid G_1 become grid nodes on a new grid G_2 . The grid G_2 has $N_{G_2} = 48252$ nodes, where $N_{G_2} = N_{G_1} + N_{E_1}$, N_{E_1} being the number of edge midpoints on grid G_1 . Every grid node on grid G_2 which is the edge midpoint on grid G_1 is marked and stored, as those grid nodes will further be used to compute the error of the DWLS reconstruction. The Navier-Stokes problem is solved numerically again by the SUPG method to obtain an accurate solution on grid G_2 . Finally, the accurate ‘true’ solution on a fine grid G_2 (Fig. 3a) is compared with the DWLS reconstruction made over a set of marked grid nodes to validate the accuracy of the DWLS approximation.

Let us introduce the error function $e(x, y)$ as follows

$$e(x, y) = |u_{SUPG}(x, y) - u_{DWLS}(x, y)|, \quad (6)$$

where we consider all points (x, y) defined by the requirement that $(x, y) \in G_2$ and (x, y) is an edge midpoint on G_1 . The function $u_{SUPG}(x, y)$ and $u_{DWLS}(x, y)$ is an accurate SUPG solution and a linearly reconstructed solution, respectively. The function $e(x, y)$ will be considered

in a computational domain D near the airfoil which is defined as a subgrid of the grid G_2 with nodes $(x, y) : \sqrt{x^2 + y^2} < R = 2.0$ (the entire domain has radius $R_f = 300.0$). The maximum error near the wall is defined as

$$e_{max} = \max_{(x, y) \in D} e(x, y). \quad (7)$$

We are also interested in the maximum error computed for the rest of domain Ω where the grid is more regular and grid cells have smaller cell aspect ratios. Namely, we compute the error

$$e_{max_1} = \max_{(x, y) \in D_1} e(x, y), \quad (8)$$

where D_1 is a subgrid of the grid G_2 with nodes $(x, y) : R_1 < \sqrt{x^2 + y^2} < R_f$, and R_1 is a chosen radius, $R_1 \geq R$.

Similarly, a logarithmic error $e^l(x, y)$ is given by

$$e^l(x, y) = \log_{10} \frac{|u_{SUPG}(x, y)|}{|u_{DWLS}(x, y)|}.$$

The maximum logarithmic error near the wall is defined as

$$e_{max}^l = \max_{(x, y) \in D} |e^l(x, y)|, \quad (9)$$

and the maximum logarithmic error in D_1 is computed as

$$e_{max_1}^l = \max_{(x, y) \in D_1} |e^l(x, y)|. \quad (10)$$

The overall accuracy of the DWLS approximation is good, as the maximum error is $e_{max_1} = 4.99432 \times 10^{-2}$ and $e_{max_1}^l = 2.32228 \times 10^{-2}$ in domain D_1 , where $R_1 = R = 2.0$. Moreover, if we consider the radius $R_1 = 10.0$, then the maximum error decreases as $e_{max_1} = 1.95457 \times 10^{-3}$ and $e_{max_1}^l = 8.50617 \times 10^{-4}$. This result can be attributed to generation of a quasiuniform grid in a far field where a DWLS method provide an accurate solution reconstruction.

Meanwhile, a DWLS reconstruction does not perform well in those grid subdomains where the stretched cells present. A grid fragment near the airfoil leading edge (domain **B** in Fig. 3a) has been selected to demonstrate the results of a

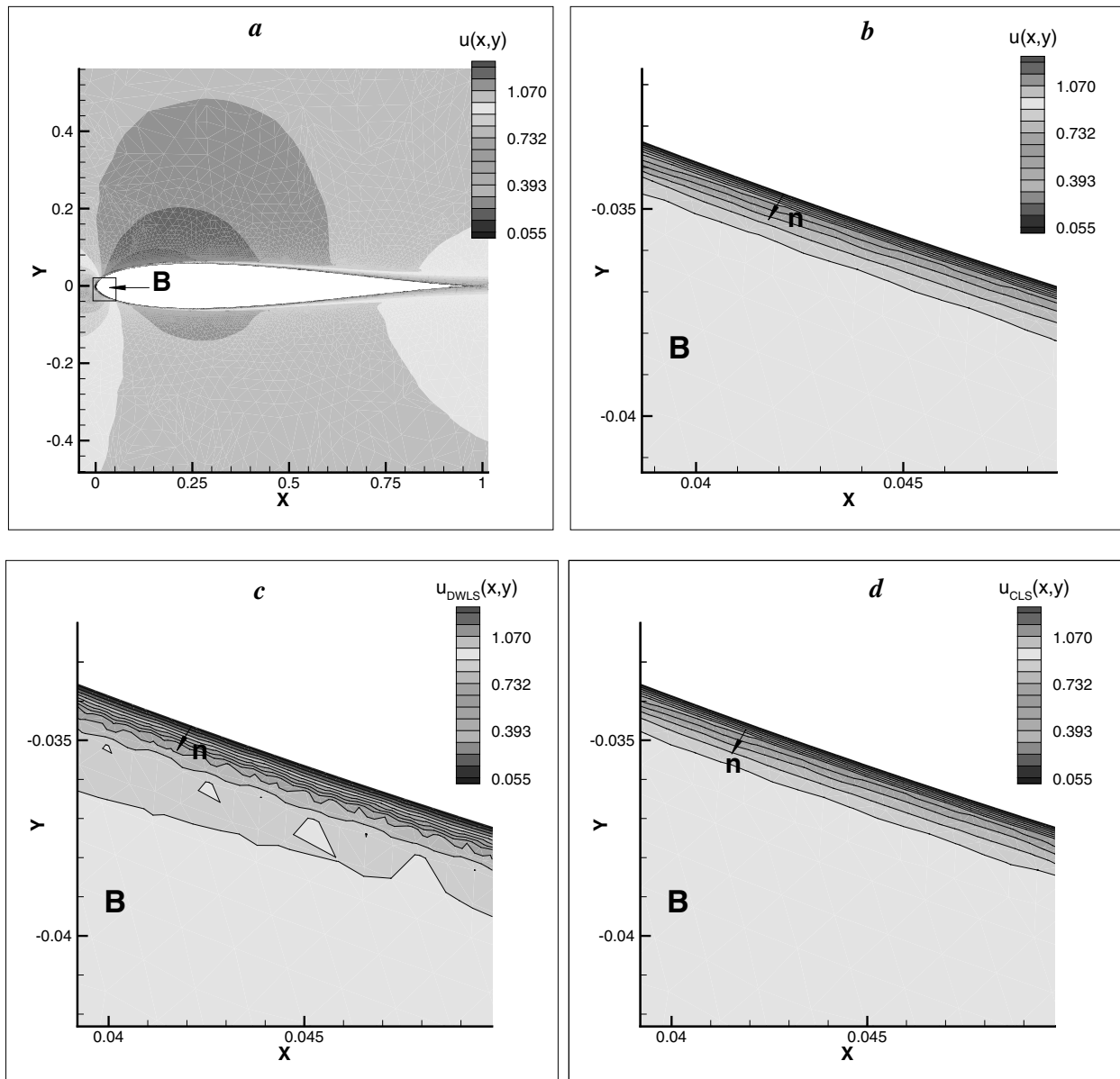


Figure 3: Results of a DWLS solution reconstruction in a computational aerodynamics problem. (a) A solution field $U(x,y)$ about an airfoil. (b) A solution close-up in the domain **B** near the wall. Solution contours are shown along with the solution colour chart. An accurate SUPG solution is a monotone function in the \mathbf{n} direction normal to the wall. (c) A DWLS reconstruction results in a non-monotone and inaccurate solution on the same grid in the domain **B**. (d) A LS reconstruction over a compact stencil S_c provides a monotone function $u_{CLS}(x,y)$.

DWLS reconstruction on cells with high cell aspect ratios. A ‘true’ SUPG solution $U(x, y)$ is presented in Fig. 3b, while a reconstructed solution $u_{DWLS}(x, y)$ is shown in Fig. 3c. It can be seen from the figure that the DWLS reconstruction results in a non-monotone and inaccurate solution near the wall.

A reconstruction error computed in the boundary layer region confirms the above result. The maximum error (7) for the linear DWLS reconstruction in domain D is

$$e_{max} \equiv e(x_0, y_0) = 0.3448,$$

where $u_{SUPG}(x_0, y_0) = 0.748121$, $u_{DWLS}(x_0, y_0) = 0.40329$, and the point (x_0, y_0) is located near the wall, $x_0 = 0.0307725$, $y_0 = -0.030712$. The maximum logarithmic error (9) for the DWLS reconstruction in a boundary layer is

$$\begin{aligned} e_{max}^l &\equiv |e^l(x_1, y_1)| = 1.85098, \\ x_1 &= 2.19748 \times 10^{-4}, \\ y_1 &= -4.52691 \times 10^{-3}, \end{aligned}$$

where $u_{SUPG}(x_1, y_1) = -3.58752 \times 10^{-3}$, $u_{DWLS}(x_1, y_1) = 5.05609 \times 10^{-5}$. Hence the DWLS reconstruction near the wall may lose several orders of magnitude degrading to unacceptably poor accuracy on stretched meshes.

The idea of weighting in a DWLS reconstruction is to allow one to effectively eliminate distant points that may be captured by a reconstruction stencil on a stretched mesh. However, an example of a DWLS reconstruction considered in this section demonstrates that the weighting of stencil points is not always efficient on grids with big cell aspect ratios. This conclusion is confirmed by other authors [Mavriplis (2003); Smith, Barone, Bond, Lorber, and Baur (2007)] who have shown in their work that introducing weights in a LS procedure has not always resulted in a more accurate reconstruction on stretched meshes. Thus our next goal is to discuss why a weighting procedure does not improve the accuracy of the DWLS approximation.

3 The problem of outliers

We have already mentioned in the previous section that weight functions used in a DWLS method are in many cases functions of the Euclidean distance between two given points. Thus data weighting is helpful when it is required to eliminate geometrically distant points from a reconstruction stencil. Many authors, therefore, advocate the data weighting on unstructured grids as they believe weighting of stencil points will result in a more accurate reconstruction [Barth (1991); Haselbacher (2006); Ollivier-Gooch, Van Alena (2002)]. However, contrary to that popular opinion, a weighting procedure will not be always efficient on stretched meshes because another type of distant points also presents in the data set. Namely, our further discussion of a DWLS reconstruction on irregular meshes is based on the assumption that a reconstruction stencil on such meshes may include numerically distant points that lie beyond the solution "range of interest". While those numerically distant points significantly affect the accuracy of the DWLS method, they can be located close to the origin P_0 in a geometric domain, in which case they cannot be eliminated by means of simple geometric weighing.

For a given function $U(x, y)$, we will name geometrically distant points as \mathbf{r} -outliers and numerically distant points will be referred to as U -outliers. The detection of U -outliers is a difficult task, as it requires a rigorous definition of a geometric domain S_l , which size will depend on properties of function $U(x, y)$. At the same time, numerical examples can be readily designed that illustrate the concept of U -outliers for a DWLS reconstruction. Below we discuss one instructive example that demonstrates a difference between geometrically distant points and numerically distant points in a reconstruction stencil.

3.1 Numerically distant points in a reconstruction stencil

Consider a quadratic function,

$$U(x, y) = 0.5((x - A)^2 - (y - A)^2), \quad (11)$$

where parameter A is taken as $A = 10$. The function (11) is reconstructed at the origin $P_0 = (0, 0)$

by a DWLS method with the inverse distance weight function (4). Let a linear polynomial function (5) be used for the reconstruction over the following stencil shown in Fig. 4a,

$$\begin{aligned} P_1 &= (0.01, -0.1), & P_2 &= (0.11, -0.01), \\ P_3 &= (-0.01, 0.08), & P_4 &= (-0.11, 0.08), \\ P_5 &= (1, 1), & P_6 &= (-0.8, -2). \end{aligned}$$

We are interested in the reconstruction error,

$$e(P_0) = |U(P_0) - u_{DWLS}(P_0)|, \quad (12)$$

and the gradient error,

$$e_{\nabla}(P_0) = \|\nabla U(x, y) - \nabla u_{DWLS}(x, y)\|_{|P_0}, \quad (13)$$

at the origin, where the gradient vector in (13) is $\nabla = (\partial/\partial x, \partial/\partial y)$. The both errors will be computed for an unweighted DWLS reconstruction, where we take $p = 0$ in the function (4), and for a weighted reconstruction with $p = 1$. For the unweighted approximation the function error and gradient error is $e(P_0) = 2.4148 \times 10^{-2}$, $e_{\nabla}(P_0) = 1.78745$, respectively. This result can be attributed to the presence of two distant points, P_5 and P_6 , in the reconstruction stencil (see Fig. 4a). Thus we expect a smaller error for a weighted reconstruction, as data weighting will mitigate the impact of distance points on the accuracy of the reconstruction. The implementation of weights in the problem gives $e(P_0) = 2.75142 \times 10^{-4}$ and $e_{\nabla}(P_0) = 5.3598 \times 10^{-3}$.

We now consider an exponential function,

$$U(x, y) = 2x^2 + \exp(2By), \quad (14)$$

with parameter $B = 3$. Let us design a reconstruction stencil that does not contain any geometrically distant points. Namely, we require that $x_i^2 + y_i^2 = R^2$ for any stencil point $P_i, i = 1, \dots, 6$, where the radius R is taken $R = 0.8$ in our computations. The stencil points are then stationed at the circumference C_R as follows (see Fig. 4b),

$$\begin{aligned} P_1 &= (-0.798, -0.056), & P_2 &= (0.798, -0.056), \\ P_3 &= (0.792, 0.112), & P_4 &= (-0.792, 0.112), \\ P_5 &= (0, 0.8), & P_6 &= (0, -0.8). \end{aligned}$$

As in the previous test case, we compute the reconstruction error (12) and the gradient error (13) at the origin. The errors for the unweighted reconstructions are $e(P_0) = 20.3738$ and $e_{\nabla}(P_0) = 69.2418$, respectively.

It is obvious that the implementation of the weight function (4) in the problem will result in the same error values, as the weights are given by $w(r_{0i}) = 1/R^p = \text{const}$ for all stencil points by the definition of stencil S_l . Meanwhile, if we eliminate points P_5 and P_6 from the reconstruction stencil, we will get an essentially smaller error, $e(P_0) = 1.1892$, $e_{\nabla}(P_0) = 1.5401$, over a new stencil $S_l = \{P_1, P_2, P_3, P_4\}$. Hence, the points P_5 and P_6 , which are not geometrically distant stencil points, can be considered as U -outliers in the problem, and we conclude that the domain S_l bounded by the circumference C_R is not adequate to the exponential function (14).

A simple evaluate of the size of domain S_l for functions (11) and (14) can be obtained from the following consideration. Let us approximate the function gradient at the origin as

$$\begin{aligned} \frac{\partial U}{\partial x} \Big|_{P_0} &\approx \tilde{\nabla}_x = \frac{U(\Delta x, 0) - U(0, 0)}{\Delta x}, \\ \frac{\partial U}{\partial y} \Big|_{P_0} &\approx \tilde{\nabla}_y = \frac{U(0, \Delta y) - U(0, 0)}{\Delta y}, \end{aligned} \quad (15)$$

where we assume that the first order approximation (15) gives us the upper bound for the gradient error. For the function (11) we have

$$\begin{aligned} \frac{U(\Delta x, 0) - U(0, 0)}{\Delta x} &= \frac{1}{2}\Delta x - A, \\ \frac{U(0, \Delta y) - U(0, 0)}{\Delta y} &= A - \frac{1}{2}\Delta y. \end{aligned}$$

The gradient at the origin is $\frac{\partial U}{\partial x} \Big|_{P_0} = \nabla_x = -A$, $\frac{\partial U}{\partial y} \Big|_{P_0} = \nabla_y = A$, and the error for each gradient component is given by

$$\begin{aligned} e_x &= |\nabla_x - \tilde{\nabla}_x| = \frac{1}{2}|\Delta x|, \\ e_y &= |\nabla_y - \tilde{\nabla}_y| = \frac{1}{2}|\Delta y|. \end{aligned} \quad (16)$$

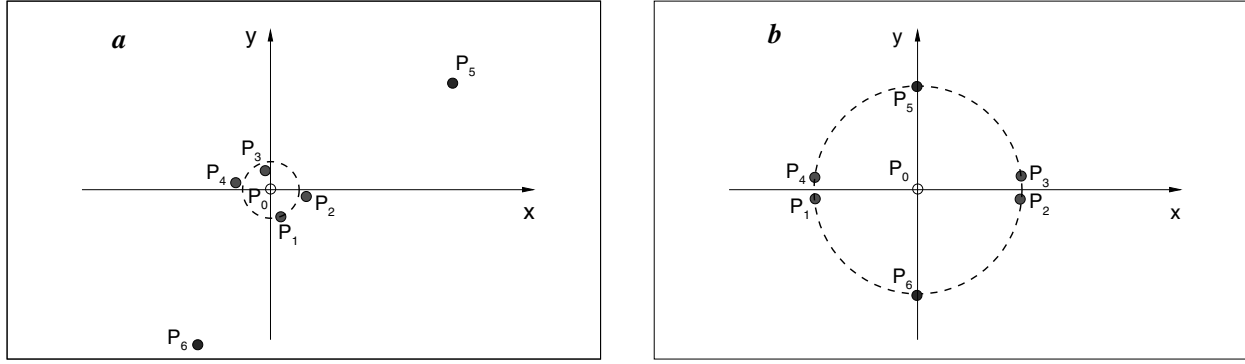


Figure 4: A reconstruction stencil for (a) an ‘isotropic’ and (b) an ‘anisotropic’ function. (a) Geometrically distant points P_5 and P_6 are also numerically distant points for the harmonic function (11). (b) Points P_5 and P_6 are numerically distant points for exponential function (14), but they are not geometrically distant points.

For the function (14) the evaluate (15) gives

$$\begin{aligned} \frac{U(\Delta x, 0) - U(0, 0)}{\Delta x} &= 2\Delta x, \\ \frac{U(0, \Delta y) - U(0, 0)}{\Delta y} &= \frac{\exp(2B\Delta y) - 1}{\Delta y} \\ &\approx 2B + 4B^2\Delta y, \end{aligned}$$

and the error for each gradient component is

$$e_x = 2|\Delta x|, \quad e_y = 4B^2|\Delta y|. \quad (17)$$

While a more accurate error estimate should involve a rigorous LS method formulation, simple evaluates (16), (17) allow us to conclude about a characteristic size of the domain S_l where stencil points should belong to. Let us require that

$$e_x = e_y = E, \quad (18)$$

so that the function derivatives will be reconstructed with the same accuracy in both directions. For a chosen length $\Delta x = l$, which is dictated by the size of grid cells on a given computational grid, we can obtain the length Δy from the condition (18). The stencil point $P_i = (x_i, y_i)$ is then considered as a distant point in the reconstruction stencil, if we have at least one of the following evaluates

$$x_i \gg \Delta x \text{ or } y_i \gg \Delta y. \quad (19)$$

For the function (11) the condition (18) determines the size of domain S_l as $\Delta x \approx \Delta y$ for

all stencil points. Thus the points P_5 and P_6 are outliers in the reconstruction stencil designed for function (11), as those geometrically distant points are numerically distant points as well. Meanwhile, for the function (14) we have $\Delta y \approx \Delta x/2B^2$, and the stencil points P_5 and P_6 , for which $x_i = y_i$, $i = 5, 6$, are outliers that should be eliminated or be stationed close to the origin according to the estimate (17).

The functions (11) and (14) present two extreme cases of an ‘isotropic’ function that needs a uniform distribution of stencil points and an ‘anisotropic’ function with a strong gradient that requires grid refinement in the y -direction. These model cases demonstrate that elimination of stencil points should not be entirely based on the geometric shape of the stencil, as the function properties should be taken into account as well. Apparently, if the distance $r_{0i} \rightarrow \infty$, then the conditions (19) are true, and the point P_i is an outlier. However the definition (19) may not agree with a simple geometric evaluation of P_i . In particular, we have seen that for the anisotropic function (14) a small distance r_{0i} may be beyond the solution domain of interest (19) if any of the lengths Δ_x and Δ_y is small. In the latter case the point P_i should be eliminated from a reconstruction stencil, despite it can be located close to the origin.

3.2 *U-outliers in a boundary layer region*

The results of the section 3.1 lead us to the conclusion that *U*-outliers may present a serious difficulty for a DWLS method as they cannot be removed by means of geometric weighting of stencil points. In this section we consider the results of a DWLS reconstruction with various degrees p of weight function (4) to demonstrate that in practical computations *U*-outliers remain in a boundary layer, no matter how heavily distant points are weighted. We also consider an extreme case of a weighted reconstruction, which is a LS reconstruction over a compact stencil. Namely, in case that a solution function should be reconstructed at the edge midpoints of a computational grid, a compact stencil $S_c = \{P_1, P_2, P_3, P_4\}$ is defined as a set of grid nodes belonging to the two grid cells that share a given edge (see stencil *II* in Fig. 2).

The reconstruction over compact stencil S_c can be considered as a weighted reconstruction on original stencil S_l where points P_i , $i = 1, \dots, 4$ have weights $w_i = 1$ and the rest of stencil points have infinitely small weights. A reconstruction over a compact stencil seems to be a controversial approach, as we miss the solution information provided by neighboring nodes when we reduce the support S_l to the set S_c . However, using a compact stencil may help one to eliminate potential *U*-outliers from the reconstruction, as neighboring nodes in reconstruction stencil S_l may appear as *U*-outliers that contaminate the results of a DWLS reconstruction. Thus we expect the maximum error for the reconstruction over a compact stencil to be compatible or even better than that for a weighted reconstruction over a standard stencil S_l . On the other hand, a reconstruction over a compact stencil does not always eliminate *U*-outliers from the stencil. For instance, if we consider a compact stencil $S_c = \{P_1, P_3, P_5, P_6\}$ for the geometry of Fig. 4b, the points P_5 and P_6 still remain *U*-outliers as it has been discussed in section 3.1. In the latter case a big reconstruction error on a compact stencil will indicate that a computational grid generated in the problem does not resolve an "anisotropic" solution function that has two characteristic lengths.

We are now going back to a Zhukovsky airfoil test

case considered previously in section 2.3 where a strongly irregular mesh was generated near the airfoil, while the mesh was quasiuniform in a far field region. The results of a DWLS reconstruction a region D near the airfoil ($R < 2.0$) are shown in Table 1. In the table we compute the maximum error (7) and the maximum logarithmic error (9) for various degrees p of polynomial weight function (4). It can be seen from the table that weighting of stencil nodes does not significantly decrease the error of the reconstruction. Moreover, the logarithmic error e_{max}^l is bigger then the error e_{max} . That result, in our opinion, indicates that the solution is not well resolved on a given grid. In other words, insertion of new nodes is required to make a grid cell size in the direction normal to the wall (the solution gradient direction) adequate to the solution characteristic length (see the discussion in section 3.1).

The last column labeled *CS* in the table is a LS reconstruction on a compact stencil where the weights are taken as $w_i = 1$ at points P_i , $i = 1, \dots, 4$. While reduction of a reconstruction stencil to a 4-point support makes a reconstruction error smaller, a compact reconstruction stencil still contains *U*-outliers, which is indicated by a relatively big logarithmic error. At the same time it is worth noticing here that, despite leaving the maximum error big, the use of a compact stencil allows one to smoothen a solution in many grid cells in a boundary layer region and to result in a monotone function as one moves normal to the airfoil boundary. A typical example of a reconstructed solution on a compact stencil is shown in Fig.3d. A reconstructed solution $u_{CLS}(x, y)$ is a monotone function, while a DWLS reconstruction using a standard reconstruction stencil results in a non-monotone solution $u_{DWLS}(x, y)$ (see Fig.3c), as it has been discussed in section 2.3.

The results of a DWLS reconstruction in a far field ($R_1 = 10.0$) are quite different from that near the airfoil. The DWLS reconstruction error is presented in Table 2 where both maximum error (8) and maximum logarithmic error (10) are computed in the far field for various degrees p . The reconstruction on a compact stencil (*CS*) is shown as the last column in the table. A DWLS recon-

Table 1: The reconstruction error for a DWLS approximation near the airfoil ($R < 2.0$). The maximum error (7) and the maximum logarithmic error (9) are shown for various degrees p of polynomial weight function (4).

p	0	1	2	4	8	CS
e_{max}	0.37684	0.36355	0.344832	0.32259	0.321201	0.305658
e_{max}^l	2.06805	1.64364	1.85098	1.37883	1.52484	1.49584

struction provides much better results in a far field region where we do not expect numerically distant points. It can be seen from the table that the logarithmic error e_{max}^l is smaller than the error e_{max} that means a well resolved solution on a given grid. At the same time, it is interesting to notice that heavy weighting of reconstruction data ($p=4$ and $p=8$) does not result in a smaller reconstruction error. Similarly, using a compact stencil in a far field does not significantly improve the results of the reconstruction.

Finally, let us mention that a quadratic reconstruction ($M = 5$ in the expansion (1)) that usually requires a greater number of stencil points is often considered as an alternative way to get a more accurate reconstruction in case that the accuracy of a linear approximation is not sufficient for a given problem [Barth (1991); Haselbacher (2006); Ollivier-Gooch, Nejat, Michalak (2007)]. Hence a common approach would be to increase a number of stencil points and to use a quadratic reconstruction on an expanded stencil in a boundary layer region. Meanwhile the results of our study of a quadratic reconstruction on stretched meshes [Petrovskaya (2008)] reveal that an expanded reconstruction stencil may provide even a bigger number of U -outliers than that for a linear approximation, so that we have to expect even worse accuracy when we use a higher order reconstruction in the problem. For instance, in the above test case the maximum error for a quadratic DWLS reconstruction with the weight function $p = 2$ is $e_{max} \equiv e(x_0, y_0) = 1.38595$, where $u_{SUPG}(x_0, y_0) = -0.0389462$, $u_{DWLS}(x_0, y_0) = 1.34701$. Similarly, the maximum logarithmic error for a quadratic DWLS reconstruction is $e_{max}^l \equiv |e^l(x_1, y_1)| = 2.48118$, where point $x_1 = 0.00668591$, $y_1 = -0.0140429$, and $u_{SUPG}(x_1, y_1) = -5.41308 \times$

10^{-2} , $u_{DWLS}(x_1, y_1) = -1.78758 \times 10^{-4}$ in a boundary layer. Thus the conclusions about accuracy of a higher order LS reconstruction should be revised if irregular meshes are exploited in the problem.

4 Concluding remarks

In the present work we have considered the problem of local approximation by a weighted least-squares method that does not require to assemble global approximation from local fit functions defined at each sub-domain of a computational grid. The method has been referred to as a discontinuous weighted least-squares (DWLS) approximation. The need to study a DWLS approximation came from computational aerodynamics applications where a DWLS method is widely used for a local solution reconstruction. It has been shown in our paper that a DWLS method cannot be considered as a reliable means of solution reconstruction on stretched meshes, as the method may degrade to unacceptable accuracy. Moreover, examples of a DWLS reconstruction discussed in the paper demonstrate that the weighting of stencil points is not efficient on stretched meshes, as it does not improve the accuracy of the method.

A concept of numerically distant points (U -outliers) has been introduced in the paper in order to reveal the nature of the accuracy problem on stretched meshes. This concept allows one to explain poor performance of the DWLS method on grids with high cell aspect ratios. A common inverse distance weighting procedure only eliminates geometrically distant points from a reconstruction stencil, while numerically distant points still remain in the stencil and may significantly affect the accuracy of the method. That

Table 2: The reconstruction error for a DWLS approximation in a far field ($R_1 = 10.0$). The maximum error (8) and the maximum logarithmic error (10) are shown for various degrees p of polynomial weight function (4).

p	0	1	2	4	8	CS
e_{max_1}	2.038×10^{-3}	1.853×10^{-3}	1.772×10^{-3}	1.954×10^{-3}	2.099×10^{-3}	1.772×10^{-3}
e'_{max_1}	8.872×10^{-4}	8.065×10^{-4}	7.712×10^{-4}	8.506×10^{-4}	9.136×10^{-4}	7.713×10^{-4}

makes weighting inefficient for those reconstruction stencils where the location of U -outliers is not directly related to the distance to a given stencil point. In the latter case it may appear to be helpful to minimize the number of stencil points in order to a priori eliminate U -outliers from the stencil. A simple procedure implemented in the paper has demonstrated that using a compact stencil may potentially be advantageous in subdomains where the solution has a strong gradient and requires a stretched mesh for its proper resolution. However, this approach requires a further thorough study and cannot currently be recommended for practical applications.

By now we do not have a reliable algorithm for an optimal choice of a reconstruction stencil in computations in unstructured meshes. Ideally such an algorithm should be based on a rigorous definition of U -outliers in a problem. Let us notice that the problem of outliers is well known in the statistics [Agee, Turner (1982); Neter, Wasserman, Kutner (1985); Press, Flannery, Teukolsky, and Vetterling (1996)] and the methods of their detection have been developed in statistical problems [Moore, McCabe (1999); Neter, Wasserman, Kutner (1985)]. Those methods, however, are not applicable in a DWLS problem, as they usually require a big data array, while it is unlikely that a reconstruction stencil on an unstructured computational grid will contain more than several dozens of grid nodes. Thus detection of numerically distant points remains the most important problem for a DWLS solution reconstruction on irregular grids.

There is one more point worth mentioning here. A usual procedure of verification of a numerical method is to consider model test cases where analytical solution is available and to compare a nu-

merical solution with the analytical one. In our paper, however, we have used 'real-life' test cases where an analytical solution was not known. That was done mainly to demonstrate difficulties arising in practical computations but also because it is very hard to design a meaningful test case, where a closed-form solution is available, in order to discuss U -outliers on stretched meshes. The matter is that if an analytical solution can be used in the problem, then all information about the solution function becomes available at the stage of computational grid generation/adaptation, so that a grid can be readily generated to take that information into account. Thus a reconstruction stencil on an adequately resolved grid would not contain numerically distant points, despite the grid itself can be strongly stretched to accommodate the solution features. In other words, U -outliers appear on grids that are not adequate to the solution (e.g., a coarse grid that does not properly resolve a boundary layer solution). Hence, in our opinion, a comprehensive approach to the problem of U -outliers in a DWLS reconstruction should be combined with a grid adaptation problem. That will consist a topic of future work on DWLS approximation.

Acknowledgments

This research was supported by The Boeing Company under contract 66-ZB-B001-10A-533. The author gratefully acknowledges discussions with Dr Forrester Johnson of Boeing who provided valuable input for this work.

References

Atluri, S.N.; Kim, H.-G.; Cho, J.Y. (1999): A Critical Assessment of The Truly Meshless Local

Petrov-Galerkin (MLPG) and Local Boundary Integral Equation (LBIE) Methods. *Computational Mechanics*, vol. 24, pp.348-372.

Agee, W.S.; Turner, R.H. (1982): Robust Range Measurement Preprocessing. *Tech. Report, National Range Operations Directorate, White Sands Missile Range NM.*

Alexa, M.; Behr, J; Cohen-Or,D; Fleishman,S; Levin,D.; T. Silva, C. (2003): Computing and Rendering Point Set Surfaces. *IEEE Transactions on Visualization and Computer Graphics*, vol.9(1), pp.3-15.

Anderson, W.K. (1994): A Grid Generation and Flow Solution Method for the Euler Equations on Unstructured Grids. *J. Comput. Phys.* vol.110(1), pp.23–38.

Anderson, W.K.; Bonhaus, D.L. (1994): An Implicit Upwind Algorithm for Computing Turbulent Flows on Unstructured Grids. *Computers and Fluids*, vol.23(1), pp.1-21.

Barth, T.J. (1991): A Three-Dimensional Upwind Euler Solver for Unstructured Meshes. *AIAA 91-1548.*

Barth, T.J.; Jespersen, D.C. (1989): The Design and Application of Upwind Schemes on Unstructured Meshes. *AIAA 89-0366.*

Bates, D.M.; Watts, D.G. (1988): Nonlinear Regression Analysis and its Applications. *New York: Wiley.*

Björck, A. (1996): Numerical Methods For Least-Squares Problems. *SIAM Philadelphia.*

Breitkopf, P.; Naceur, H.; Rassineux, A.; Villon, P. (2005): Moving Least Squares Response Surface Approximation: Formulation and Metal Forming Applications Methods. *Computers and Structures*. vol.83, pp.1411-1428.

Haselbacher, A. (2006): On Constrained Reconstruction Operators. *AIAA 2006-1274.*

Haselbacher, A.; Vasilyev, O.V. (2003): Commutative Discrete Filtering on Unstructured Grids Based on Least-Squares Techniques. *J. Comput. Phys.*, vol.187(1), pp.197-211.

Hughes, T.J.R.; Brooks, A. (1979): A Multi-dimensional Upwind Scheme with no Crosswind Diffusion. In: *Finite Element Methods for Convection Dominated Flows.* New York, ASME.

Johnson, F.T. (2007): Boeing Test Cases for a Higher Order Least-Squares Reconstruction. *Personal communication.*

Lancaster,P; Salkauskas, K. (1981): Surfaces Generated by Moving Least Squares Methods. *Mathematics of Computation*, vol.37(155), pp.141–158.

Levin, D. (1998): The Approximation Power of Moving Least-Squares. *Math. Comput.* vol.67(224), pp.1517-1531.

Mavriplis, D.J. (2003): Revisiting the Least - Square Procedure for Gradient Reconstruction on Unstructured Meshes. *AIAA 2003-3986.*

Mavriplis, D.J. (2007): Unstructured Mesh Discretizations and Solvers for Computational Aerodynamics. *AIAA 2007-3955.*

Moore, D. S.; McCabe, G. P. (1999): Introduction to the Practice of Statistics, 3rd ed. New York: W. H. Freeman.

Most, T.; Bucher, C. (2008): New Concepts for Moving Least Squares: An Interpolating Non-Singular Weighting Function and Weighted Nodal Least Squares. *Engineering Analysis with Boundary Elements*, vol.32, pp.461-470.

Nayroles, B.; Touzot, G.; Villon, P. (1992): Generalizing the FEM: Diffuse Approximations and Diffuse Elements. *Computational Mechanics*, vol.10, pp.307-318.

Nie, Y.F.; Atluri, S.N.; Zou, C.W. (2006): The Optimal Radius of the Support of Radial Weights Used in Moving Least Squares Approximation. *CMES: Computer Modeling in Engineering & Science*, vol.12(2), pp.137-147.

Neter, J.; Wasserman, W.; Kutner, M.H. (1985): Applied Linear Statistical Models. Richard D. Irwin, Inc., Illinois.

Ollivier-Gooch, C.; Van Altena, M. (2002): A High-Order-Accurate Unstructured Mesh Finite-Volume Scheme for the Advection-Diffusion Equation. *J. Comp. Phys.*, vol.181, pp.729–752.

Ollivier-Gooch, C.; Nejat, A.; Michalak, K. (2007): On Obtaining High-Order Finite-Volume Solutions to the Euler Equations on Unstructured Meshes. *AIAA 2007-4464*.

Perko, J.; Šarler, B. (2007): Weight Function Shape Parameter Optimization in Meshless Methods for Non-Uniform Grids. *CMES: Computer Modeling in Engineering & Science*, vol.19(1), pp.55-68.

Petrovskaya, N.B. (2007): Some Issues of Implementation of Higher Order Schemes in Computational Aerodynamics. *Boeing technical report 66-ZB-B001-10A-533, The Boeing Company, Seattle, USA*.

Petrovskaya, N.B. (2008): A Quadratic Least-Squares Solution Reconstruction in a Boundary Layer Region. (submitted)

Prax, C.; Sadat, H.; Dabboura, E. (2007): Evaluation of High Order Versions of the Diffuse Approximate Meshless Method. *Applied Mathematics and Computation*, vol.186(2), pp.1040-1053.

Prax, C.; Salagnac, P., Sadat, H. (1998): Diffuse Approximation and Control-Volume-Based Finite-Element Methods: A Comparative Study. *Numerical Heat Transfer B*, vol.34, pp.303-321.

Press, W.H.; Flannery, B.P.; Teukolsky, S.A.; Vetterling, W.T. (1996): *Numerical Recipes in Fortran 77: The Art of Scientific Computing*. Cambridge University Press.

Sadat, H.; Prax, C. (1996): Application of the Diffuse Approximation for Solving Fluid Flow and Heat Transfer Problems. *International Journal of Heat and Mass Transfer*, vol.39(1), pp.214-218.

Šarler, B.; Vertnik, P.; Perko, J. (2005): Application of Diffuse Approximate Method in Convective-Diffusive Solidification Problems. *Computers, Materials & Continua*, vol.2, pp.77-83.

Smith, T.; Barone, M.; Bond, R.; Lorber, A.; Baur, D. (2007): Comparison of Reconstruction Techniques for Unstructured Mesh Vertex Centered Finite Volume Schemes. *AIAA 2007-3958*.

Venkatakrishnan, V.; Allmaras, S.R.; Johnson, F.T.; Kamenetskii, D.S. (2003): Higher Order Schemes for the Compressible Navier-Stokes Equations. *AIAA 2003-3987*.

Wendland, H. (1995): Piecewise Polynomial, Positive Definite and Compactly Supported Radial Basis Functions of Minimal Degree. *Adv. Comput. Math.*, vol.4, pp.389-396.